Symmetric and dissymmetric pyrazolyl-bridged rhodium dimers. Two X-ray dirhodium structures with short metal–metal interactions

C. López [a], J.A. Jiménez [a], R.M. Claramunt [a,*], M. Cano [b,*], J.V. Heras [b], J.A. Campo [b], E. Pinilla [b], A. Monge [c]

[a] Departamento de Química Orgánica y Biología, Facultad de Ciencias, UNED, Senda del Rey s / n, 28040-Madrid, Spain
[b] Departamento de Química Inorgánica I, Facultad de Ciencias Químicas, Universidad Complutense, 28040-Madrid, Spain
[c] Instituto de Ciencias de los Materiales sede D, CSIC, Serrano 113, Laboratorio de Difracción de Rayos-X, Cristalografía, Facultad de Químicas, Universidad Complutense, 28040-Madrid, Spain

Abstract

The molecular structure of complexes [{Rh(μ-pz *)(NBD)}$_2$] (1a–7a) and [{Rh(μ-pz *)(CO)$_2$}$_2$] (1b–7b) (pz * = pyrazolate, 3,5-dimethylpyrazolate, 3(5)tert-butylpyrazolate, 3-methyl-5-tert-butylpyrazolate, 3(5)-phenylpyrazolate, 3-methyl-5-phenylpyrazolate and 3(5)-p-methoxyphenylpyrazolate) has been studied by IR and ^{1}H and ^{13}C NMR spectroscopies. ^{1}H NMR variable temperature experiments were also carried out. We also report the crystalline structure of two complexes isolated as unique configurational isomers, [{Rh(μ-bupz)(NBD)}$_2$] · CH$_2$Cl$_2$ · H$_2$O (3a), and [{Rh(μ-mbupz)(NBD)}$_2$] · CH$_2$Cl$_2$ (4a).

1. Introduction

The pyrazolate groups as bridging ligands have been extensively used in dimetallic homo- and hetero-nuclear complexes involving Rh and Ir. One of the main reasons is interest in the cooperative influence of neighbouring metal centres on catalytical reactions [1].

Most of the work described deals with iridium dimers [{Ir(pz *)(COD)}$_2$] [2–4] and the aim of this work was to prepare new rhodium complexes [{Rh(μ-pz *)(NBD)}$_2$], (1a–7a), (μ-pz * = pyrazolate, 3,5-dimethylpyrazolate, 3(5)tert-butylpyrazolate, 3-methyl-5-tert-butylpyrazolate, 3(5)-phenylpyrazolate, 3-methyl-5-phenylpyrazolate and 3(5)-p-methoxyphenylpyrazolate and NBD = (2.3.5.6-η)-bicyclo[2.2.1]hepta-2,5-diene), and to explore the effect that changes in the pyrazole substituents, in the metal and in the ancillary ligand would have on skeletal and metal–metal interactions. Finally, their behaviour towards CO was also studied.

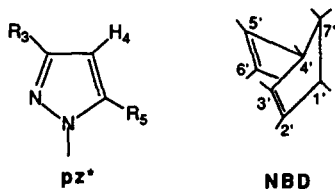NMR studies at different temperatures to establish the solution structures and the crystalline structure of two complexes, [{Rh(μ-bupz)(NBD)}$_2$] (3a) and [{Rh(μ-mbupz)(NBD)}$_2$] (4a) isolated as unique configurational isomers are reported.
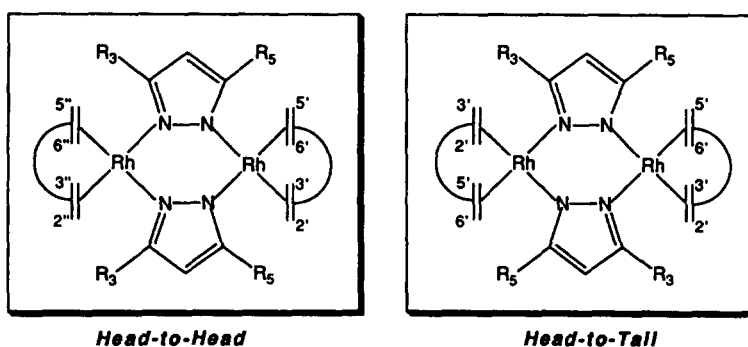
2. Experimental section

In spite of the use of the Schlenk techniques in previous work, we have found that it was not necessary to carry out the reactions in an inert atmosphere. The reactions were performed at room temperature. Commercial solvents were dried prior to use. Syntheses of the starting Rh-complex and the ligands have been described previously: [{Rh(μ-Cl)(NBD)}$_2$] [5], 3(5)-tert-butylpyrazole (Hbupz) [6], 3(5)-phenylpyrazole (Hphpz) [6], 3(5)-p-methoxyphenylpyrazole (Hph * pz) [7] and 3-methyl-5-phenylpyrazole (Hmphpz) [8]. Pyrazole (Hpz) and 3,5-dimethylpyrazole (Hdmpz) were commercial and used without further purification.

Elemental analyses for carbon, hydrogen and nitrogen were carried out by the Microanalytical Service of the Complutense University. IR spectra were recorded

---

* Corresponding authors.

Scheme 1.

on a Perkin–Elmer 1300 spectrometer in KBr discs. ^{1}H-NMR spectra were performed on a Varian XL-300 (299.95 MHz) and on a Bruker AC-200 (200.13 MHz) spectrometer. The ^{13}C-NMR spectra were recorded on the latter spectrometer working at 50.33 MHz. Chemical shifts δ are listed in parts per million relative to tetramethylsilane; coupling constants J are in hertz. The ^{1}H and ^{13}C chemical shifts are accurate to 0.01 and 0.1

ppm respectively. Coupling constants are accurate to ±0.2 Hz for ^{1}H NMR spectra and ±0.6 Hz for ^{13}C NMR spectra.

The NMR spectra at various temperatures were taken with the Bruker spectrometer in a 5 mm dual probe with $CDCl_3$ and $(CD_3)_2CO$ as solvents. The temperature of the probe was calibrated by the methanol standard method, and a delay of 600 s was used before register-

Table 1
IR data, colour, isolated yield and elemental analyses of complexes 1a–7a

Complex	IR (cm^{-1}) [a]	Colour	Yield (%)	Molecular formula	Calc.			Found		
					C	H	N	C	H	N
[{Rh(μ-pz)(NBD)}$_2$] (1a)	1300	yellow	83	$C_{20}H_{22}N_4Rh_2$	45.81	4.24	10.69	45.39	4.12	10.19
[{Rh(μ-dmpz)(NBD)}$_2$] (2a)	1300	orange	95	$C_{24}H_{30}N_4Rh_2$	49.66	5.22	9.65	48.78	5.06	8.94
[{Rh(μ-bupz)(NBD)}$_2$] (3a)	1300	orange-red	96	$C_{28}H_{38}N_4Rh_2$	52.83	6.03	8.80	52.68	5.66	8.40
[{Rh(μ-mbupz)(NBD)}$_2$] (4a)	1300	orange	76	$C_{30}H_{42}N_4Rh_2$	54.21	6.38	8.43	53.91	6.00	8.03
[{Rh(μ-phpz)(NBD)}$_2$] (5a)	1300	red	89	$C_{32}H_{30}N_4Rh_2$	56.81	4.48	8.28	56.63	4.34	7.80
[{Rh(μ-mphpz)(NBD)}$_2$] (6a)	1300	orange-red	81	$C_{34}H_{34}N_4Rh_2$	57.96	4.87	7.95	57.74	5.18	7.44
[{Rh(μ-ph* pz)(NBD)}$_2$] (7a)	1305	orange-red	92	$C_{34}H_{34}O_2N_4Rh_2$	55.44	4.66	7.61	55.25	4.53	7.37

[a] β(CH)

Table 2
IR data, colour, isolated yield and elemental analyses of complexes 3b–7b

Complex	IR (cm^{-1}) [a]	Colour	Yield (%)	Molecular formula	Calc.			Found		
					C	H	N	C	H	N
[{Rh(μ-bupz)(CO$_2$)}$_2$] (3b)	2080 2060 2010 2000sh	yellow	78	$C_{18}H_{22}O_4N_4Rh_2$	38.31	3.94	9.93	38.03	3.75	9.62
[{Rh(μ-mbupz)(CO$_2$)}$_2$] (4b)	2080 2060 2000 1975sh	yellow	84	$C_{20}H_{26}O_4N_4Rh_2$	40.55	4.43	9.46	39.98	4.22	9.09
[{Rh(μ-phpz)(CO$_2$)}$_2$] (5b)	2080 2065 2010 2000sh	yellow	82	$C_{22}H_{14}O_4N_4Rh_2$	43.73	2.34	9.27	43.26	2.43	8.86
[{Rh(μ-mphpz)(CO$_2$)}$_2$] (6b)	2090 2060 2000 1995sh	yellow	75	$C_{24}H_{18}O_4N_4Rh_2$	45.59	2.88	8.86	45.30	2.66	8.45
[{Rh(μ-ph * pz)(CO)$_2$}$_2$] (7b)	2090 2070 2020 2005sh	yellow	77	$C_{24}H_{18}O_6N_4Rh_2$	43.39	2.74	8.44	42.77	2.56	7.81

[a] ν(CO); sh = shoulder.

Table 3
Crystal and refinement data for [{Rh(μ-bupz)(NBD)}$_2$] · CH$_2$Cl$_2$ · H$_2$O (3a) [{Rh(μ-mbupz)(NBD)}$_2$] · CH$_2$Cl$_2$ (4a)

	(3a)	(4a)
Formula	$N_4C_{29}H_{42}Cl_2Rh_2O$	$N_4C_{31}H_{44}Cl_2Rh_2$
Mr	739.39	749.44
Crystal system	monoclinic	tetragonal
Space group	$P2_1/c$	$I\bar{4}2d$
a (Å)	11.737(2)	25.581(3)
b (Å)	12.18(1)	–
c (Å)	22.238(3)	9.897(3)
β (deg)	98.63(1)	–
V (Å^3)	3143(3)	6478(2)
Z	4	8
F(000)	1504	3056
ρ (calc.) (g cm^{-3})	1.56	1.54
Temp. (K)	295	295
μ (cm^{-1})	12.3	11.9
Crystal dimensions (mm)	0.2 × 0.4 × 0.2	0.3 × 0.3 × 0.4
Diffractometer	Enraf–Nonius CAD4	Enraf–Nonius CAD4
Radiation	graphite-monochromated Mo K α (λ = 0.71069 Å)	graphite-monochromated Mo K α (λ = 0.71069 Å)
Scan technique	ω–2θ	ω–2θ
Data collected	(−13, 0, 0) to (13, 14, 26)	(0, 0, 0) to (30, 30, 11)
θ	1 < θ < 25	1 < θ < 25
Unique data	5515	1615
Unique data $(I) \geq 2\sigma(I)$	3542	1251
R(int) (%)	0.8	1.7
Std. rflns.	3/228	3/273
R_F (%)	5.8	3.1
Rw_F (%)	6.9	3.3
Average shift/error	0.41	0.80

ing the NMR spectra at each temperature. INEPT sequences and the 2D experiments were carried out in the usual manner [9].

2.1. Preparation of [{Rh(μ-pz*)(NBD)}₂]

To a suspension of [{Rh(μ-Cl)(NBD)}₂] (0.2 mmol) in methanol (15 ml) was added the corresponding pyrazole (0.4 mmol). To the clear orange-yellow solution immediately formed was added a solution of KOH in methanol (5 ml) in aliquots of 1 ml during a period of 30 s, and an orange-red solid precipitated. The mixture was stirred for 15 min and then the solid was filtered off, washed with cold methanol and dried in vacuo. Yields are given in Table 1.

2.2. Preparation of [{Rh(μ-pz*)(CO)₂}₂]

Carbon monoxide was bubbled for 10–30 min through a solution of [{Rh(μ-pz*)(NBD)}₂] in

dichloromethane (15 ml) at room temperature and atmospheric pressure. The initial orange-red of the solution changed to yellow. The yellow residue obtained by evaporation was treated with diethyl ether and evaporated again to dryness. The yellow solid was washed with cold hexane and dried in vacuo. Yields are given in Table 2.

2.3. X-ray structure determination

Single red octahedral crystals of [{Rh(μ-bupz)-(NBD)}₂] · CH₂Cl₂ · H₂O, **3a** and [{Rh(μ-mbupz)-(NBD)}₂] · CH₂Cl₂, **4a** were obtained from dichloromethane–hexane.

The data were collected on an Enraf–Nonius CAD4 diffractometer for both compounds, and unit cell constants were refined from least squares fitting of the θ values of 25 reflections. A summary of the fundamental crystal data for both crystals are given in Table 3, and

Table 4
Atomic coordinates and thermal parameters as $U_{eq} = 1/3\Sigma_i\Sigma_j U_{ij} a_i^* a_j^* \mathbf{a}_i \cdot \mathbf{a}_j \times 10^4$ for non-hydrogen atoms of (3a)

Atom	x	y	z	U_{eq}
Rh1	0.17584(8)	0.37116(8)	0.66716(4)	391(3)
Rh2	0.35074(8)	0.18375(8)	0.70413(4)	369(3)
N11	0.1253(8)	0.2169(8)	0.6349(5)	425(33)
N12	0.2020(7)	0.1320(8)	0.6439(4)	390(31)
C13	0.1489(9)	0.0413(9)	0.6188(5)	386(38)
C14	0.037(1)	0.068(1)	0.5929(6)	548(47)
C15	0.026(1)	0.178(1)	0.6038(6)	501(43)
C16	0.203(1)	−0.072(1)	0.6211(6)	480(43)
C17	0.164(1)	−0.137(1)	0.6726(7)	713(57)
C18	0.160(1)	−0.130(1)	0.5604(7)	702(59)
C19	0.334(1)	−0.066(1)	0.6292(7)	620(53)
N21	0.3179(8)	0.3640(8)	0.6216(4)	420(32)
N22	0.3980(8)	0.2828(8)	0.6339(4)	391(32)
C23	0.482(1)	0.302(1)	0.5997(5)	485(44)
C24	0.454(1)	0.395(1)	0.5648(6)	595(53)
C25	0.352(1)	0.432(1)	0.5796(6)	522(46)
C26	0.593(1)	0.234(1)	0.6041(7)	611(54)
C27	0.574(1)	0.115(1)	0.6191(7)	630(55)
C28	0.635(2)	0.239(1)	0.5413(7)	938(78)
C29	0.683(1)	0.285(2)	0.6527(8)	822(68)
C31	0.228(1)	0.498(1)	0.7298(6)	542(48)
C32	0.174(1)	0.543(1)	0.6769(7)	611(52)
C33	0.047(1)	0.552(1)	0.6845(7)	648(55)
C34	0.014(1)	0.430(1)	0.6820(7)	629(53)
C35	0.070(1)	0.384(1)	0.7355(6)	529(47)
C36	0.136(1)	0.477(1)	0.7709(6)	535(46)
C37	0.055(1)	0.575(1)	0.7525(7)	648(56)
C41	0.441(1)	0.275(1)	0.7756(6)	539(47)
C42	0.502(1)	0.181(1)	0.7680(6)	557(47)
C43	0.463(1)	0.096(1)	0.8106(6)	638(54)
C44	0.341(1)	0.075(1)	0.7770(6)	595(53)
C45	0.280(1)	0.168(1)	0.7845(5)	530(47)
C46	0.361(1)	0.248(1)	0.8227(6)	557(48)
C47	0.438(1)	0.166(1)	0.8639(6)	659(56)
C1	0.766(2)	−0.196(2)	0.5083(7)	913(74)
CL1	0.6818(5)	−0.0932(5)	0.5304(3)	1251(22)
CL2	0.8481(6)	−0.2544(6)	0.5683(2)	1407(25)
O1	0.9099(9)	0.0734(8)	0.0074(5)	1053(49)

Table 5
Atomic coordinates and thermal parameters as $U_{eq} = 1/3\Sigma_i\Sigma_j U_{ij} a_i^* a_j^* \mathbf{a}_i \cdot \mathbf{a}_j \times 10^3$ for non-hydrogen atoms of (4a)

Atom	x	y	z	U_{eq}
Rh1	0.77566(3)	0.06030(3)	0.73474(8)	44(1)
N1	0.7108(3)	0.0116(3)	0.7516(10)	50(3)
N2	0.6872(3)	0.0095(3)	0.8759(10)	49(3)
C3	0.6462(4)	−0.0239(4)	0.8670(13)	55(4)
C4	0.6443(4)	−0.0432(5)	0.7390(14)	68(4)
C5	0.6858(5)	−0.0204(4)	0.6687(11)	59(4)
C6	0.6098(4)	−0.0357(5)	0.9840(17)	78(5)
C7	0.5680(4)	0.0080(6)	0.9872(19)	111(6)
C8	0.6392(5)	−0.0386(6)	1.1173(14)	75(5)
C9	0.5824(6)	−0.0883(6)	0.9615(18)	126(7)
C10	0.7034(5)	−0.0299(5)	0.5273(12)	77(5)
C51	0.7371(5)	0.1281(5)	0.6747(14)	73(5)
C52	0.7527(6)	0.1008(5)	0.5608(12)	81(5)
C53	0.8052(5)	0.1237(5)	0.5224(13)	78(5)
C54	0.8373(4)	0.1021(5)	0.6408(15)	71(5)
C55	0.8212(4)	0.1285(4)	0.7520(14)	63(4)
C56	0.7792(6)	0.1666(5)	0.7065(12)	76(5)
C57	0.7988(7)	0.1811(6)	0.5636(13)	93(6)
CL	0.7574(2)	−0.1537(1)	0.7307(5)	116(2)
C1	0.7500(0)	−0.1156(7)	0.8750(0)	80(7)

Table 6
^{1}H NMR data of complexes 1a–7a (200 MHz) at 298 K

Compound	Pyrazole protons			NBD protons			Solvent
	R_3	H_4	R_5	CH-2′,3′,5′,6′	CH-1′,4′	CH$_2$-7′	
[{Rh(μ-pz)(NBD)}$_2$] (1a)	6.86(d) $J_{34} = J_{45} = 2.0$	6.03(t)	6.86(d)	← 3.87–3.92 (m, 12H) →		1.55 (br s, 4H)	CDCl$_3$
[{Rh(μ-dmpz)(NBD)}$_2$] (2a)	2.27(s)	5.44(s)	2.27(s)	4.34 (br s, 8H)	4.02 (br s, 2H) 4.34 (br s, 2H)	1.56 (br s, 4H)	CDCl$_3$
[{Rh(μ-bupz)(NBD)}$_2$] (3a)	7.14(d) $J_{34} = 1.9$	5.83(d)	1.43(s)	← 3.8–4.5 (br m, 12H) →		1.43 (s, 4H)	CDCl$_3$
	7.14(d) $J_{34} = 2.0$	5.77(d)	1.40(s)	4.15 (br s, 8H)	3.96 (br s, 2H) 4.44 (br s, 2H)	1.40 (s, 4H)	(CD$_3$)$_2$CO
[{Rh(μ-mbupz)(NBD)}$_2$] (4a)	2.47(s)	5.47(s)	1.39(s)	4.18 (2H, H$_{2'}$) 4.75 (2H, H$_{3'}$) 4.24 (2H, H$_{5'}$) 4.53 (2H, H$_{6'}$)	3.98 (2H, H$_{1'}$) 4.45 (2H, H$_{4'}$)	1.44 (br s, 4H)	CDCl$_3$
[{Rh(μ-phpz)(NBD)}$_2$] (5a) [a]	7.26(br s)	6.28(br s)	8.37(br s)H$_o$ 7.56(m)H$_m$ 7.42(m)H$_p$	← 3.27–4.30 (m, 24H) →		1.16–1.42 (m, 8H)	CDCl$_3$
	7.30(d) $J_{34} = 1.9$	6.27(d)	8.44(m)H$_o$ 7.57(m)H$_m$ 7.41(m)H$_p$	← 3.0–4.5 (m, 24H) →		1.15–1.45 (m, 8H)	(CD$_3$)$_2$CO
[{Rh(μ-mphpz)(NBD)}$_2$] (6a) [b]	2.48(s)	5.96(s)	8.38(d, 7.8)H$_o$ 7.52(t)H$_m$ 7.38(d,7.5)H$_p$	4.51 (2H, H$_{2'}$) 4.25 (2H, H$_{3'}$) 4.16(2H, H$_{5'}$) 3.37(2H, H$_{6'}$)	3.77 (2H, H$_{1'}$) 4.27 (2H, H$_{4'}$)	1.13–1.45 (br m, 4H)CDCl$_3$	
	2.43(s)	5.94(s)	8.48(m)H$_o$ 7.54(m)H$_m$ 7.36(m)H$_p$	4.61(2H); 4.39(2H); 4.31(2H) 4.23(2H); 3.79(2H); 3.35(2H)		1.5–1.4 (br m, 4H)	(CD$_3$)$_2$CO
[{Rh(μ-ph* pz)(NBD)}$_2$] (7a) [c]	7.21(br s)	6.18(s)	8.26(br s)H$_o$ 7.08(d, 8.3)H$_m$ 3.93(s)-OMe	← 3.2–4.4 (br m, 24H) →		1.0–1.5(br m, 8H)	CDCl$_3$

br s = broad signal; br m = broad multiplet; s = singlet; d = doublet; t = triplet; m = multiplet.
[a] Compound 5a is a mixture of 60%/40% isomers (ratio determined at 253 K in (CD$_3$)$_2$CO and at 223 K in CDCl$_3$).
[b] Compound 6a is a mixture of 20% H-H/80% H-T isomers (ratio determined at 298 K) and only the data for the major isomer are reported. The assignment of the signals was made on the basis of homonuclear (^{1}H–^{1}H) COSY and NOESY experiments and heteronuclear (^{1}H–^{13}C) correlation.
[c] Compound 7a is a mixture of 60%/40% isomers (ratio determined at 253 K).

Table 7

^{1}H NMR data at variable temperature for [{Rh(μ-bupz)(NBD)}$_2$] (3a) in (CD$_3$)$_2$CO

Temperature (K)	CH-1′ CH-4′	CH-2′,6′	CH-3′,5′	CH-1″ CH-4″	CH-2″,6″	CH-3″,5″
328	3.97 (2H)	4.16 (2H)	4.16 (2H)	4.45 (2H)	4.16 (2H)	4.16 (2H)
203	4.02 (1H) 3.85 (1H)	4.02 (2H)	4.38 (2H)	4.59 (1H) 4.28 (1H)	4.21 (2H)	3.91 (2H)

the final values of all refined atomic coordinates in Tables 4 and 5.

The intensities were corrected for Lorentz and polarization effects. Scattering factors for neutral atoms and anomalous dispersion corrections for Rh and Cl were taken from the International Tables for X-ray Crystallography [10].

Both structures were solved by Patterson and Fourier methods. Empirical absorption corrections [11] were applied at the end of the isotropic refinements. The maximum and minimum absorption correction factors were 1.065 and 0.880 for 3a and 1.170 and 0.808 for 4a.

For [{Rh(μ-bupz)(NBD)}$_2$] · CH$_2$Cl$_2$ · H$_2$O 3a some non-resolvable disorder from thermal motion has been found for the Cl atoms of the dichloromethane molecule, and because of this, these atoms have been refined only isotropically. Final mixed refinement with unit weights

and fixed coordinates and isotropic thermal factors for the hydrogen atoms lead to $R = 5.8\%$.

For [{Rh(μ-mbupz)(NBD)}$_2$] · CH$_2$Cl$_2$, 4a, final mixed refinement with unit weights employed fixed coordinates and the isotropic thermal factors for the hydrogen atoms, lead to $R = 3.1\%$. No trend in ΔF vs F_0 or (sin θ)/λ were observed.

Most of the calculations were carried out with the X-ray 80 program [12]. Full lists of atomic coordinates, thermal parameters and bond lengths and angles have been deposited at the Cambridge Crystallographic Data Centre.

3. Results and discussion

Reaction of the chloro-bridged dimer [{Rh(μ-Cl)(NBD)}$_2$] with a stoichiometric amount of Hpz*

Table 8

^{13}C{^{1}H} NMR data of complexes 3a–7a ^{a} in CDCl$_3$ (50 MHz) at 298 K

Compound		C$_3$	C$_4$	C^5	R	NBD carbons
[{Rh(μ-bupz)(NBD)}$_2$] ^{b}	(3a)	136.8	101.2	161.0	^{t}Bu: 31.7; 31.5	C$_{7'}$: 62.0; J_{Rh} = 5.8 C$_{2',3',5',6'}$: 56.0–59.5 (v br s) C$_{1',4'}$: 51.2; J_{Rh} = 2.8
[{Rh(μ-mbupz)(NBD)}$_2$]	(4a)	145.2	100.1	161.6	Me: 14.5 ^{t}Bu: 31.7; 31.6	C$_{7'}$: 62.6; J_{Rh} = 5.8 C$_{2'}$: 52.9; J_{Rh} = 10.2 C$_{3'}$: 57.5; J_{Rh} = 10.4 C$_{5'}$: 58.1; J_{Rh} = 9.2 C$_{6'}$: 60.8; J_{Rh} = 9.8 C$_{1'}$: 50.9; J_{Rh} = 2.6 C$_{4'}$: 51.3; J_{Rh} = 2.5
[{Rh(μ-phpz)(NBD)}$_2$]	(5a)	138.1	103.7	151.2	Ph: 134.5; 128.1 127.1; 127.0	C$_{7'}$: 61.9; J_{Rh} = 5.7 C$_{2',3',5',6'}$: 57.0–59.2 (br m) C$_{1',4'}$: 50.5–51.5 (br m)
[{Rh(μ-mphpz)(NBD)}$_2$] ^{c}	(6a)	147.7	103.2	151.2	Me: 14.0 Ph: 135.0; 127.9 127.1; 126.9	C$_{7'}$: 62.3; J_{Rh} = 6.0 C$_{2'}$: 57.5; J_{Rh} = 9.8 C$_{3'}$: 57.3; J_{Rh} = 9.3 C$_{5'}$: 59.5; J_{Rh} = 9.4 C$_{6'}$: 59.1; J_{Rh} = 9.8 C$_{1'}$: 51.4; J_{Rh} = 2.7 C$_{4'}$: 50.9; J_{Rh} = 2.5
[{Rh(μ-ph* pz)(NBD)}$_2$]	(7a)	137.9	103.1	150.9	Ph*: 158.0; 128.1 127.5; 113.5 –OMe: 55.4	C$_{7'}$: 61.9; J_{Rh} = 5.3 C$_{2',3',5',6'}$: 57.0–59.3 (br m) C$_{1',4'}$: 50.5–51.5 (br m)

v br s = very broad signal; br m = broad multiplet. ^{a} Complexes 1a and 2a were too insoluble to record the ^{13}C NMR spectra. ^{b} At 323 K. ^{c} Typical coupling constant values (J in Hz) are: Me, ^1J = 126.5; C$_4$-pz, ^1J = 172.5; Ph carbons, NBD carbons: ^1J = 158.4; C$_{1',4'}$; ^1J = 155.8; C$_{2',3',5',6'}$, ^1J = 183.8; C$_{7'}$, ^1J = 132.5.

(Hpz* = pyrazole, 3,5-dimethylpyrazole, 3(5)-*tert*-butylpyrazole, 3-methyl-5-*tert*-butylpyrazole, 3(5)-phenylpyrazole, 3-methyl-5-phenylpyrazole and 3(5)-*p*-methoxyphenylpyrazole) in methanol solution and with the addition of potassium hydroxide leads to the dinuclear complexes [{Rh(μ-pz*)(NBD)}$_2$], (**1a–7a**), as air-stable yellow or orange-red solids in nearly quantitative yield (Eq. (1)). The compounds were characterized by elemental analyses, IR spectra (Table 1) and ^{1}H and ^{13}C NMR data (Tables 6, 7 and 8) and they behave as neutral species in solution.

$$[\{Rh(\mu\text{-Cl})(NBD)\}_2] + 2Hpz^*$$

$$\xrightarrow{2KOH} [\{Rh(\mu\text{-pz}^*)(NBD)\}_2] + 2KCl + 2H_2O$$

$$(1)$$
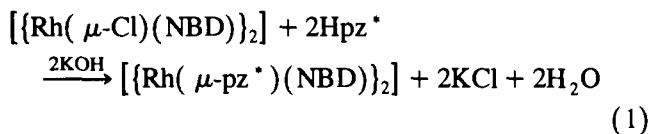
Owing to the unsymmetrical substitution of the bridging ligands, other than pyrazole and 3,5-dimethylpyrazole, the dinuclear complexes [{Rh(μ-pz*)(NBD)}$_2$] can exist as two geometrical isomers: the two bridges can be oriented head-to-head (H-H) with a C_s symmetry or head-to-tail (H-T) having a C_2 symmetry axis (Scheme 1).

Surprisingly, in the case of 3-*tert*-butylpyrazole only the H-H configuration was obtained, whereas for 3-methyl-5-*tert*-butylpyrazole the H-T isomer was the unique compound isolated. The remaining pyrazoles afforded mixtures of both configurations, H-H and H-T, in different proportions, corresponding to the degree of steric hindrance (see Table 6). Similar results have been reported by Elguero et al. [13a] for [{Rh(μ-3(5)-methylpz)(COD)}$_2$] and by Bushnell et al. [4] for [{Ir(μ-pz*)(COD)}$_2$]. The ratio of H-H/H-T isomers was determined by ^{1}H NMR spectroscopically at low temperature by integration of the resonances of the ortho-protons of the aryl groups which were clearly resolved into two doublets; at 298 K only a broad signal was observed for these protons.

The ^{1}H and ^{13}C spectra of derivative **4a** are compatible with the H-T isomer in which the central six-membered ring Rh$_2$N$_4$ exists in a boat conformation. The diolefin moiety gives rise to seven NBD signals at room temperature. The assignment was performed using homonuclear (^{1}H–^{1}H) COSY and NOESY experiments (Fig. 1). The 7'-methylene protons appeared at δ 1.44 and were coupled with two tertiary protons of δ 3.98 (H$_{1'}$) and 4.45 (H$_{4'}$). The olefinic 2'-CH at δ 4.18 and the olefinic 6'-CH at δ 4.53 showed a NOE effect with the methyl group at δ 2.47 and with the tert-butyl group at δ 1.39 respectively. Signals at δ 4.75 and 4.24 were then straightforwardly attributed to the olefinic protons 3'-CH and 5'-CH. A heteronuclear (^{1}H–^{13}C) correlation (Fig. 2) then permitted the assignment of the ^{13}C chemical shifts (Table 8), the most important feature being the upfield signal of C$_{2'}$ at δ 52.9 as a result of the steric crowding of the tert-butyl substituent.
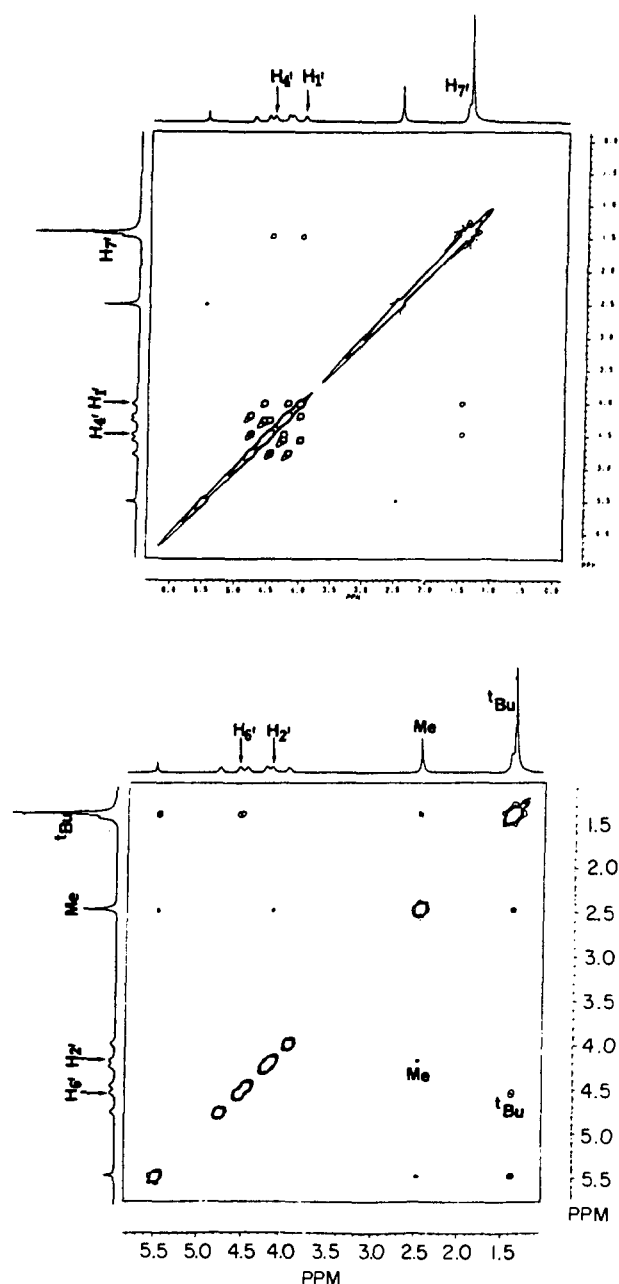

Fig. 1. (a) (^{1}H–^{1}H) COSY and (b) (^{1}H–^{1}H) NOESY experiments for [{Rh(μ-mbupz)(NBD)}$_2$] (**4a**).

In complex **3a** there are two different norbornadienes and from the coordination mode shown by the X-ray analysis; five ^{1}H and ^{13}C resonances for each NBD would be expected in the slow-exchange limit.

At room temperature (298 K) the ^{1}H NMR spectrum of **3a** shows a broad complex multiplet in CDCl$_3$ for the olefinic and aliphatic CH which converts into three sets of signals at δ 3.96 (2H, H$_{1'}$ and H$_{4'}$), 4.15 (8H) and 4.44 (2H, H$_{1''}$ and H$_{4''}$) in (CD$_3$)$_2$CO. The spectrum in CDCl$_3$ changes when the temperature is raised from 298 to 328 K, whereas the spectrum obtained in (CD$_3$)$_2$CO remains unaltered on heating. The pattern of the spectra in CDCl$_3$ at 328 K was similar to the one

observed in $(CD_3)_2CO$ at 298 K with only slight differences in the chemical shifts: δ 3.95 (2H), 4.12 (8H), 4.35 (2H).

This suggests structural fluxionality in these molecules, the recorded spectra in $CDCl_3$ at 298 K being close to the coalescence point. Variable-temperature experiments in this solvent were not conclusive, giving the following resonances at the lowest experimental temperature attained (213 K) δ 4.51 (1H), 4.19 (6H, br m), 3.97 (4H) and 3.82 (1H).

However, when the dynamic NMR experiments were carried out in $(CD_3)_2CO$ (Fig. 3) at 203 K we observed the eight expected resonances for the olefinic and aliphatic CH protons: 1′,4′-CH at δ 3.85 and 4.02, 2′-CH/6′-CH at δ 4.02, 3′-CH/5′-CH at δ 4.38; 1″-CH at δ 4.59 and 4″-CH at δ 4.28, 2″-CH/6″-CH at δ 4.21 and 3″-CH/5″-CH at δ 3.91 ppm, the asignment being made on the basis of a homonuclear (^1H–^1H) COSY experiment at that temperature. The methylene protons were hidden by the tert-butyl signal. The barrier to the dynamic process at 275 K was estimated by using the

Eyring equation [14] $\Delta G_c^\# = 4.57 \ T_c[9.97 + \log 10(T_c/\Delta\nu)]$ to be 13.4 kcal mol^{-1}, where T_c is the coalescence temperature and $\Delta\nu$ the difference in chemical shifts of the two sites; two sharp signals at low temperature (4.59–4.28 and 4.02–3.85) merge into one broad signal at higher temperature (4.45 and 3.97).

In principle, two processes could account for the NMR behaviour of 3a, the fluxionality of the norbornadiene ligands and the boat–boat flip of the $Rh(NN)_2Rh$ central ring. Preliminary extended Hückel molecular orbital (EHMO) calculations [15] on the energy barrier for the boat–boat inversion through a planar transition state in the case of similar complexes, [Rh(μ-pz*)(LL)] (pz* = 3-methylpyrazole and 3,5-dimethylpyrazole) (LL = $2C_2H_4$, COD, 2CO, $2CN^tBu$),indicate that the boat–boat flip is hindered by the methyl substituents. Consequently, the measured $\Delta G_c^\#$ probably corresponds to rotational motions of the diolefin ligands. Cocivera et al. pointed out that this exchange phenomenon appears to be enhanced by donor ligands [16].

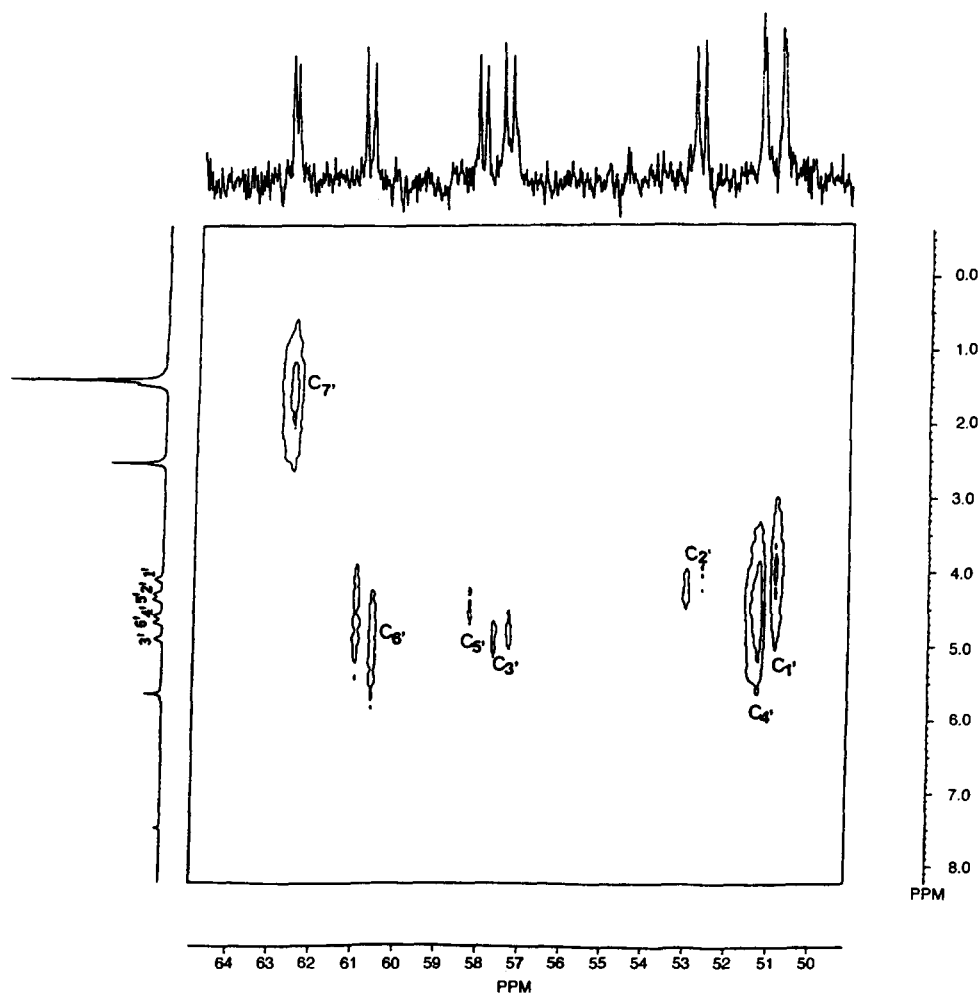Related fluxional processes have been proposed for

Fig. 2. The ^{13}C–^1H heteronuclear correlation experiment for [{Rh(μ-mbupz)(NBD)}$_2$] (4a).

boat-boat inversion

Scheme 2.
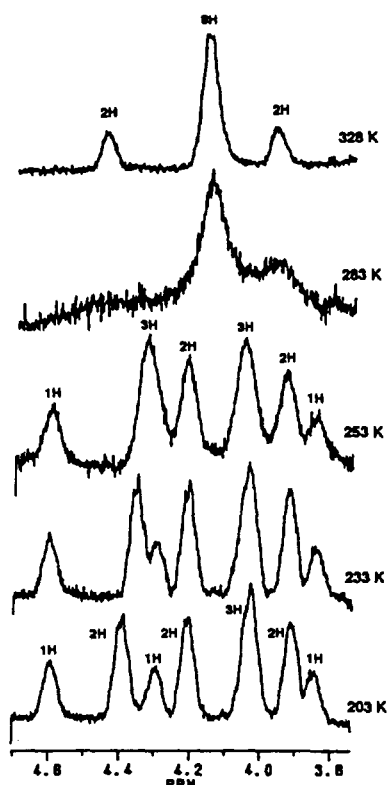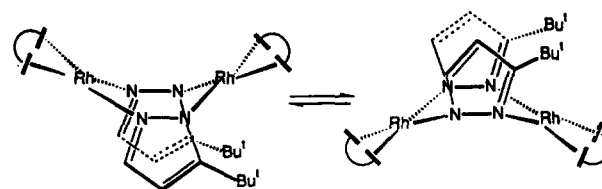

Fig. 3. ^{1}H NMR variable-temperature spectra in $(CD_3)_2CO$ for (3a).

poly(pyrazolyl)borate complexes of tin(II) and lead(II) [17] and in rhodium complexes of types [{Rh(μ-pz)Cl-(CN^{t}Bu)$_2$}$_2$(μ-CHR)] [18] and [Rh{Ph$_2$Bpz$_2$}(LL)] (LL = 2CO, NBD, COD) [19].

The syntheses of the tetracarbonyl derivatives [{Rh(μ-pz*)(CO)$_2$}$_2$] (1b-7b) involved the reaction between [{Rh(μ-pz*)(NBD)}$_2$] and carbon monoxide in dichloromethane. The complexes were isolated as yellow crystals and their purity was ascertained by elemen-

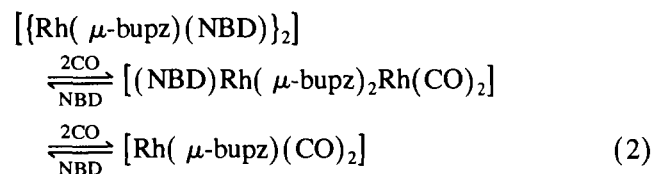tal analyses (3b-7b in Table 2). Complexes 1b and 2b had already been reported [13].

In the case of [{Rh(μ-bupz)(CO)$_2$}$_2$] (3b) our attempts to isolate this species from the solution containing the displaced norbornadiene yielded a mixture of 3b together with the mixed-complex [(NBD)Rh(μ-bupz)$_2$Rh(CO)$_2$] due to the equilibria in Eq. (2) [20]:

$$[\{Rh(\mu\text{-bupz})(NBD)\}_2]$$

$$\overset{2CO}{\underset{NBD}{\rightleftharpoons}} [(NBD)Rh(\mu\text{-bupz})_2Rh(CO)_2]$$

$$\overset{2CO}{\underset{NBD}{\rightleftharpoons}} [Rh(\mu\text{-bupz})(CO)_2] \qquad (2)$$

[{Rh(μ-mbupz)(CO)$_2$}$_2$] (4b) is a single compound and 5b-7b were mixtures of H-H and H-T isomers with ratios determined for the starting materials [{Rh(μ-pz*)(NBD)}$_2$] (5a-7a), as shown in the ^{1}H NMR spectra (Table 9).

The X-ray crystal structure of [{Rh(μ-bupz)-(NBD)}$_2$] · CH$_2$Cl$_2$ · H$_2$O (3a) confirmed the existence of a dimeric neutral species formed by two rhodium atoms, two pyrazolate rings and two norbornadiene groups.

The two rhodium atoms and the two nitrogens of the pyrazolyl rings give a metallocycle Rh(NN)$_2$Rh in a boat conformation (Fig. 4). The compound crystallized

Table 9
^{1}H NMR data of complexes 3b-7b (300 MHz) at 298 K

Compound	R$_3$	H$_4$	R$_5$
[{Rh(μ-bupz)(CO$_2$)}$_2$] (3b)	7.26(d, 1.8)	5.95(d)	1.42(s)
[{Rh(μ-mbupz)(CO$_2$)}$_2$] (4b)	2.26(s)	5.77(s)	1.38(s)
[{Rh(μ-phpz)(CO$_2$)}$_2$] (5b)	7.69(br s) (60%)	6.51(br s)(60%)	7.90(d, 7.8)H$_o$(60%)
			7.45(m)H$_m$,H$_p$(60%)
	7.62(br s)(40%)	6.51(br s)(40%)	7.99(d, 6.9)H$_o$(40%)
			7.45(m)H$_m$,H$_p$(40%)
[{Rh(μ-mphpz)(CO$_2$)}$_2$] (6b)	2.56(s)(80%)	6.28(s)(80%)	7.91(d, 7.8)H$_o$(80%)
			7.45(m)H$_m$,H$_p$(80%)
	2.45(s)(20%)	5.95(s)(20%)	7.95(d, 7.8)H$_o$(20%)
			7.45(m)H$_m$,H$_p$(20%)
[{Rh(μ-ph* pz)(CO$_2$)}$_2$] (7b)	7.66(d, 2.1)(60%)	6.43(d)(60%)	7.83(d, 8.7)H$_o$(60%)
			7.00(d)H$_m$(60%)
			3.88(s)-OMe(60%)
	7.59(d, 1.8)(40%)	6.43(d)(40%)	7.90(d, 8.7)H$_o$(40%)
			7.02(d)H$_m$(40%)
			3.91(s)-OMe(40%)

Table 10
Selected bond distances (Å) and angles (deg) [{Rh(μ-bupz)(NBD)}$_2$] · CH$_2$Cl$_2$ · H$_2$O (3a) with ESDs in parentheses

Rh1–Rh2	3.098(2)	Rh2–C41	2.10(1)
Rh1–N11	2.067(9)	Rh2–C42	2.10(1)
Rh1–N21	2.08(1)	Rh2–C44	2.11(1)
Rh1–C31	2.10(1)	Rh2–C45	2.10(1)
Rh1–C32	2.10(1)	Rh2–C4142	1.98(1)
Rh1–C34	2.11(1)	Rh2–C4445	1.99(1)
Rh1–C35	2.11(1)	C31–C32	1.37(2)
Rh1–C3132	1.99(1)	C34–C35	1.39(2)
Rh1–C3435	1.99(1)	C41–C42	1.38(2)
Rh2–N12	2.129(8)	C44–C45	1.37(2)
Rh2–N22	2.112(9)		
N11–Rh1–N21	90.1(4)	C42–Rh2–C45	80.1(5)
C34–Rh1–C35	38.5(5)	C42–Rh2–C44	67.1(5)
C32–Rh1–C35	80.5(6)	C41–Rh2–C45	67.8(5)
C32–Rh1–C34	67.8(6)	C41–Rh2–C44	80.2(5)
C31–Rh1–C35	67.2(5)	C41–Rh2–C42	38.3(5)
C31–Rh1–C34	80.1(5)	N22–Rh2–C45	150.0(5)
C31–Rh1–C32	37.9(5)	N22–Rh2–C44	167.7(5)
N21–Rh1–C35	163.1(4)	N22–Rh2–C42	102.5(4)
N21–Rh1–C34	154.3(5)	N22–Rh2–C41	95.6(5)
N21–Rh1–C32	96.5(5)	N12–Rh2–C45	96.7(4)
N21–Rh1–C31	100.3(4)	N12–Rh2–C44	99.5(5)
N11–Rh1–C35	98.6(5)	N12–Rh2–C42	162.0(5)
N11–Rh1–C34	98.3(5)	N12–Rh2–C41	155.3(5)
N11–Rh1–C32	158.9(5)	Rh1–N11–N12	119.3(7)
N11–Rh1–C31	159.3(5)	Rh2–N12–N11	109.2(7)
N12–Rh2–N22	89.2(4)	Rh1–N21–N22	120.8(7)
C44–Rh2–C45	38.0(5)	Rh2–N22–N21	108.3(7)

C3132, C3435, C4142 and C4445 are the midpoints of (C31, C32) (C34, C35) (C41, C42) and (C44, C45) respectively.

with a molecule of dichloromethane and one of water. The *tert*-butyl groups are situated in the H-H position, and both are close to Rh2. The bond lengths and angles

with their standard deviations are given in Table 10.

The crystal structure of [{Rh(μ-mbupz)(NBD)}$_2$] · CH$_2$Cl$_2$ (4a) also shows a dimeric species (Fig. 5) with

Table 11
Selected bond distances (Å) and angles (deg) [{Rh(μ-mbupz)(NBD)}$_2$] · CH$_2$Cl$_2$ (4a) with ESDs in parentheses

Rh1–Rh1'	3.071(1)	C4–C5	1.40(2)
Rh1–N1	2.083(8)	C5–C10	1.49(2)
Rh1–N2'	2.12(1)	C6–C7	1.55(2)
Rh1–C51	2.08(1)	C6–C8	1.52(2)
Rh1–C52	2.09(1)	C6–C9	1.53(2)
RH1–C54	2.12(1)	C51–C52	1.38(2)
RH1–C55	2.10(1)	C51–C56	1.49(2)
Rh1–C5152	1.97(1)	C52–C53	1.51(2)
Rh1–C5455	1.99(1)	C53–C54	1.53(2)
N1–N2	1.37(1)	C53–C57	1.53(2)
N1–C5	1.32(1)	C54–C55	1.36(2)
N2–C3	1.36(1)	C55–C56	1.52(2)
C3–C4	1.36(2)	C56–C57	1.55(2)
C3–C6	1.52(2)		
N1–Rh1–N2'	86(3)		
N1–Rh1–C5455	169(4)		
N1–Rh1–C5152	99(5)		
N2'–Rh1–C5455	104(4)		
C5152–Rh1–N2'	173(4)		
C5455–Rh1–C5152	70(5)		
C51–Rh1–C52	39(5)		
C54–Rh1–C55	37(5)		

C5152 and C5455 are the midpoints of (C51, C52) and (C54, C55) respectively. Symmetry code ('): $1\frac{1}{2} - x$, y, $1\frac{3}{4} - z$.
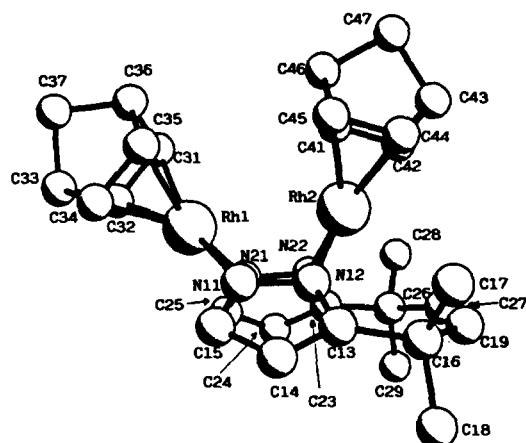
Fig. 4. A Pluto plot of **3a**. The solvent and the hydrogen atoms have been omitted for clarity.

a boat conformation of the metallocycle Rh(NN)₂Rh, similar to that found in compound **3a**, with the rhodium atoms in a square-planar coordination and the methyl and the tert-butyl groups in alternate positions. The twofold axis passes through the middle of a line between the two Rh atoms and through the C atom of the dichloromethane molecule. Table 11 shows selected bond distances and angles for this compound.

The packing of the cell is shown in Fig. 6 for both compounds **3a** and **4a**. The NBD is as expected [16,21].

In Table 12 are delineated some least squares planes passing through the atoms involved in the coordination for both **3a** and **4a**. The dihedral angles between the pyrazolato-planes (9 and 10) and the coordination planes (2 and 3) reveal that the pyrazolato-ligands lie in a position intermediate between normal and parallel to the coordination planes.

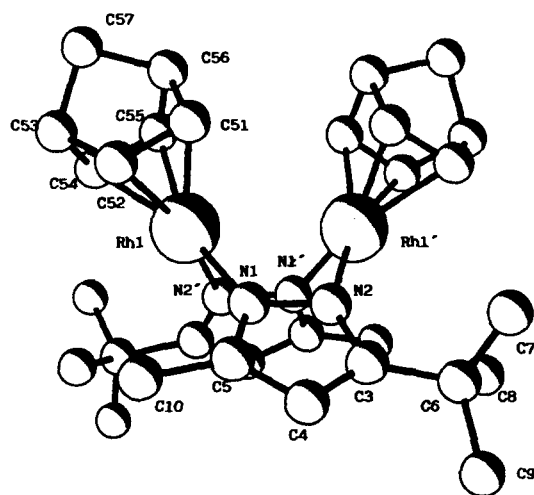The orientation of the norbornadiene in both **3a** and

Fig. 5. A Pluto plot of **4a**. The solvent and the hydrogen atoms have been omitted for clarity.
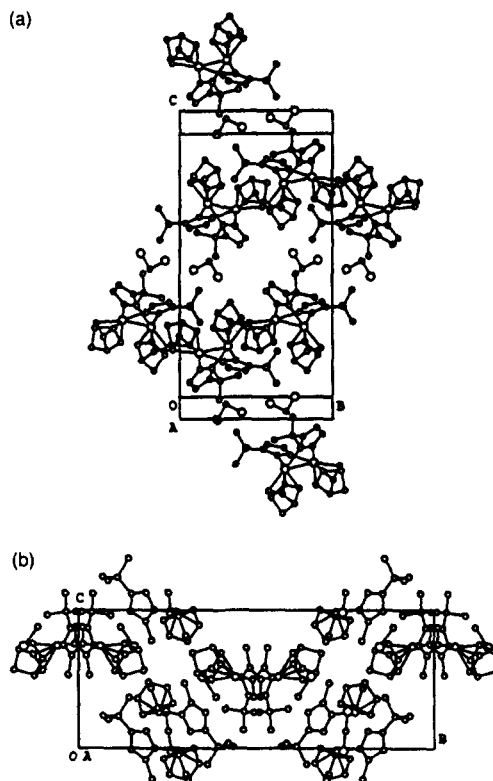
(a)

(b)

Fig. 6. Packing arrangements (a) in **3a**, (b) in **4a** viewed down the *a* axis.

4a merits further comment. From the values of dihedral angles between the planes 2-4 (92.6(5) for **3a** and 88.0(4) for **4a**) and 3-5 (82.9(4) for **3a** and 88.0(4) for **4a**), the NBD is orthogonal to the square-planar Rh coordination.

Considering the least-square plane formed by the four N atoms of the pyrazolyl rings [22], in compound **3a**, the distance from Rh2 to this plane is longer than that of Rh1, 1.334(1) and 1.058(1) Å respectively. In compound **4a** the distances are similar, 1.270(1) Å. Also, the angles between the coordination planes are 69.9(3) in **3a** and 63.8(2) in **4a**; this corresponds to the Rh1-Rh2 distances of 3.098(2) for **3a** and 3.071(1) Å for **4a**, both of them significantly shorter that of 3.267(2) found in [{Rh(μ-pz)(COD)}₂] [3].

All these geometrical features are a consequence of the different disposition of the substituents of the pyrazolate rings, H-H for **3a** and H-T for **4a**.

4. Concluding remarks

The structures and a reaction of a series of dimetallic complexes, the pyrazolyl-bridged rhodium(I) dimers of type [{Rh(μ-pz*)(NBD)}₂] (**1a-7a**) (pz* = pyrazolate (pz), 3,5-dimethylpyrazolate (dmpz), 3(5)-*tert*-butyl-pyrazolate (bupz), 3-methyl-5-*tert*-butylpyrazolate

Table 12

Selected angles (deg) between the least squares sets defined by the specified atoms for the (3a) and (4a)

(3a)	(4a)
Planes	
1-N21,N22,N12,N11	1-N1,N2,N1',N2'
2-N21,N11,C3132,C3435	2-N1,N2',C5152,C5455
3-N22,N12,C4142,C4445	3-N1',N2,C5152',C5455'
4-C31,C32,C34,C35	4-C51,C52,C54,C55
5-C41,C42,C44,C45	5-C51',C52',C54',C55'
6-Rh1,C36,C37,C33	6-Rh1,C53,C57,C56
7-Rh1,C31,C32	7-Rh1,C51,C52
8-Rh1,C34,C35	8-Rh1,C54,C55
9-N11,N12,C13,C14,C15	9-N1,N2,C3,C4,C5
10-N21,N22,C23,C24,C25	10-N1',N2',C3',C4',C5'
11-Rh2,C43,C47,C46	
12-Rh2,C41,C42	
13-Rh2,C44,C45	
1-2	44.8(4)	58.1(4)
1-3	65.3(4)	58.1(4)
1-9	34.3(4)	41.1(3)
1-10	36.2(4)	41.1(3)
2-3	69.9(3)	63.8(2)
2-4	92.6(5)	88.0(4)
2-9	52.3(3)	67.0(4)
2-10	58.0(3)	67.0(4)
3-5	82.9(4)	88.0(4)
3-9	72.0(4)	67.0(4)
3-9	66.7(3)	67.0(4)
6-7	36.1(6)	35.0(6)
6-8	35.9(6)	35.7(5)
9-10	70.4(4)	82.2(4)
11-12	36.1(4)	
11-13	35.8(4)	

Symmetry code ('): $1\frac{1}{2} - x, y, 1\frac{3}{4} - z$.

(mbupz), 3(5)-phenylpyrazolate (phpz), 3-methyl-5-phenylpyrazolate (mphpz) and 3(5)-*p*-methoxyphenyl-pyrazolate (ph* pz)) have been investigated.

The complexes containing bupz and mbupz are single configurational isomers: H-H in [{Rh(μ-bupz)(NBD)}₂] (3a) and H-T in [{Rh(μ-mbupz)(NBD)}₂] (4a). The remaining unsymmetrically substituted pyrazoles are mixtures of H-H and H-T in different proportions.

¹H and ¹³C NMR measurements in solution indicate that the 4a is stereochemically rigid in solution, but that 3a is fluxional. The ¹H NMR spectrum obtained at 203 K in (CD₃)₂CO for this latter complex reveals that the frozen structure is close to the one obtained from the X-ray structural analysis.

The X-ray data show that 3a and 4a are dimeric neutral species formed by two rhodium atoms, two pyrazolate rings and two norbornadiene groups exhibiting an Rh(NN)₂Rh metallocycle in a boat conformation with the rhodium atoms in a square-planar coordination.

Rather short intramolecular Rh–Rh distances of 3.098(2) for 3a and 3.071(1) Å for 4a were encountered, attributable to a metal–metal interaction.

5. Supplementary material available

Tables of observed and calculated structure factors for these compounds (30 pages) can be obtained from the authors.

References

[1] (a) G. Wilkinson, F.G.A. Stone and E.W. Abel (eds.), Comprehensive Organometallic Chemistry, Vol. 5, Pergamon, Oxford, 1982; (b) E.W. Abel, F.G.A. Stone and G. Wilkinson (eds.), Comprehensive Organometallic Chemistry II, Vol. 8, Elsevier, Oxford, 1995.

[2] K.A. Beveridge, G.W. Bushnell, R.R. Dixon, D.T. Eadie, S.R. Stobart, J.L. Atwood and M.J. Zawarotko, J. Am. Chem. Soc., 104 (1982) 920.

[3] K.A. Beveridge, G.W. Bushnell, S.R. Stobart, J.L. Atwood and M.J. Zawarotko, Organometallics, 2 (1983) 1447.

[4] G.W. Bushnell, D.O. Kimberley Fjeldsted, S.R. Stobart, M.J. Zaworotko, S.A.R. Knox and K.A. Macpherson, Organometallics, 4 (1985) 1107.

[5] E.W. Abel, M.A. Bennett and G. Wilkinson, J. Chem. Soc., (1959) 3178.

[6] S. Trofimenko, J.C. Calabrese and J.S. Thompson, Inorg. Chem., 26 (1987) 1507.

[7] S. Trofimenko, J.C. Calabrese, J.K. Kochi, F.B. Wolowiec, F.B. Hulsbergen and J. Reedjik, Inorg. Chem., 31 (1992) 3943.

[8] J. Elguero and R. Jacquier, Bull. Soc. Chim. Fr., (1966) 2832.

[9] W.R. Croasmun and R.M.K. Carlson, Two Dimensional NMR Spectroscopy, VCH, Weinheim, 1994.

[10] International Tables for X-ray Crystallography, Vol. 4, Kynoch, Birmingham, 1974, pp. 72-98.

[11] N. Walker and D. Stuart, Acta Crystallogr. Sect. A, 39 (1983) 158.

[12] J.M. Stewart, The X-ray 80 System, 1985 (Computer Science Center, University of Maryland, College Park, MD).

[13] (a) J. Elguero, M. Esteban, M.F. Grenier-Loustalot, L.A. Oro and M.T. Pinillos, J. Chim. Phys., 81 (1984) 251; (b) S. Trofimenko, Inorg. Chem., 10 (1971) 1372.

[14] M. Oki, Applications of Dynamic NMR Spectroscopy to Organic Chemistry, VCH, Deerfield Beach, 1985, p. 5.

[15] J.A. López, F.J. Lahoz and L.A. Oro, unpublished results.

[16] M. Cocivera, G. Ferguson, F.J. Lalor and P. Szczecinski, Organometallics, 1 (1982) 1139.

[17] D.L. Reger, Y. Ding, A.L. Rheingold and R.L. Ostrander, Inorg. Chem., 33 (1994) 4226.

[18] M.A. Ciriano, M.A. Tena and L.A. Oro, J. Chem. Soc. Dalton Trans., (1992) 2123.

[19] M. Bortolin, U.E. Bucher, H. Ruegger, L.M. Venanzi, A.

Albinati, F. Lianza and S. Trofimenko, *Organometallics, 11* (1992) 2514.

[20] (a) R. Usón, M.A. Ciriano, M.T. Pinillos, A. Tiripicchio and M. Tiripicchio Camellini, *J. Organomet. Chem.,* 205 (1981) 247; (b) R. Usón, L.A. Oro, M.A. Ciriano and M.C. Bello, *J. Organometal. Chem.,* 240 (1982) 199.

[21] P. Ballesteros, C. López, C. López, R.M. Claramunt, J.A. Jimenez, M. Cano, J.V. Heras, E. Pinilla and A. Monge, *Organometallics, 13* (1994) 189.

[22] M. Nardelli, A. Musatti, P. Domiano and G.D. Andreetti, *Ric. Sci. Part 2, Sect. A,* 8 (1965) 807.